Adsorption of Ammonia and Its Influence on Coadsorbed Carbon Monoxide on Monolayer and Multilayer Palladium Epitaxially Grown on Mo(110)

C. Xu and D. W. Goodman*

Department of Chemistry, Texas A&M University, P.O. Box 300012, College Station, Texas 77842-3012

Received: February 11, 1998; In Final Form: March 30, 1998

The adsorption of ammonia on a monolayer of Pd on Mo(110), Pd_{1ML}/Mo(110), and multilayer Pd(111)/Mo-(110) surfaces has been studied using low-energy electron diffraction (LEED), temperature-programmed desorption (TPD), and high-resolution electron energy loss spectroscopy (HREELS). A diffuse (2×2) LEED pattern has been observed for ammonia on the Pd_{1ML}/Mo(110) surface. TPD measurements indicate a shift of the desorption peak maximum of ammonia to a lower temperature for monolayer palladium compared to multilayer palladium. However, both surfaces display virtually identical HREELS spectra with the symmetric deformation (umbrella mode) being the dominating feature, indicating an upright adsorption geometry on both surfaces. The coadsorption of NH_3 and CO has been also studied with HREELS over a wide coverage range on both surfaces. A strong interaction between adsorbed NH_3 and CO is indicated by the red shift of the CO stretching vibrational mode (as large as 400 cm^{-1}) and a blue shift of the NH_3 symmetric deformation (up to 100 cm^{-1}). On Pd_{1ML}/Mo(110), the coadsorption of NH_3 induces a CO adsorption site change from the atop site to the three-hollow site. Evidence has been also found for a significantly inclined NH_3 molecule in the coadsorbed layer with a relatively high CO coverage.

1. Introduction

The chemistry of bimetallic surfaces has received considerable attention in recent years due to the novel properties exhibited by these systems relative to their single-component counterparts.[1−5] Palladium monolayers supported on early transition metals are the most studied systems of this kind.[1−17] It has been found that a palladium monolayer has a reduced ability to adsorb CO, H_2, and C_2H_4 compared to bulk palladium.[6−18] There is some controversy in the literature regarding the origin of the modified properties of supported monolayer transition metals on dissimilar metals. Systematic studies have been carried out to address the correlation between the adsorption behavior of a supported metal overlayer toward CO and its electronic structure.[1,4,5] The change in the binding energy of CO on a number of supported metal monolayers has been correlated with the XPS core level shifts of the metal overlayer as well as work function changes.[4,5] A simple model has been advanced to explain the reduced binding energy of a Pd monolayer on early transition metal: the depletion of 4d electron density through charge polarization from Pd toward the metal substrate and the rehybridization of the Pd(4d,5s,5p) levels.[1,5]

Unlike CO, NH_3 is a weak donor ligand, which adsorbs on the surface through the nitrogen lone pair electrons in a single dative bond. It is instructive to compare these two different bonding mechanisms, especially multilayer palladium relative to monolayer palladium. The adsorption of NH_3 on transition-metal surfaces is also of considerable interest because of its relevance to ammonia synthesis. In recent years, the catalytic de-NO_x process using NH_3 has also received considerable attention. The interaction of ammonia with NH_3-synthesis-relevant surfaces, such as Fe and Ru, has been extensively characterized using a number of surface science techniques (refs 19−21 and references therein). These studies have been extended to other surfaces including Pt(111),[22−24] Ni(111),[25−28] Ni(110),[29−30] Ag(110),[31] Ag(311),[32] Al(111),[33] and NiO(100).[34] However, no studies have been carried out on palladium surfaces or any ultrathin metal overlayers. In this paper, we report on our recent studies of adsorption of NH_3 on palladium monolayers supported on the Mo(110) surface and a Pd(111) surface epitaxially grown on the Mo(110) surface.

The second focus of this paper is the coadsorption of NH_3 with CO on these surfaces. The coadsorption of NH_3 and CO has been studied previously on Ni(111),[35−38] Ni(110),[36,37] Ru-(001),[39,40] Re(0001),[41] and Cu(110)[42] surfaces. Using metastable quenching spectroscopy (MQS), Tochihara et al.[35] have studied the coadsorption of NH_3 and CO on Ni(111). These authors found that NH_3 on top of a CO layer leads to an increase in the back-donation from the metal substrate into the $2\pi^*$ orbital of CO. The adsorption of NH_3 on top of CO chemisorbed on Ni-(111) and Ni(110) has been studied by Dresser et al.[34] and Lanzillotto et al.,[37] using electron-stimulated desorption ion angular distribution (ESDIAD) and temperature-programmed desorption (TPD). A short-range CO−NH_3 interaction was found on Ni(111) with the C_{3v} axis of NH_3 inclined away from the surface normal. Erley[38] has studied the coadsorption of NH_3 and CO on Ni(111) using infrared spectroscopy. Zhou et al.[39] and Sakaki et al.[40] studied NH_3 and CO coadsorption on Ru-(001) using high-resolution electron energy loss spectroscopy (HREELS), low-energy electron diffraction (LEED), and TPD, and they showed that CO coadsorbed with NH_3 induces a red shift in the C−O stretching vibrational mode. Mijoule et al.[43] have carried out density functional calculations of the vibrational stretching mode of CO coadsorbed with NH_3 on Pd clusters. Their calculations showed that the C−O stretching frequency, the CO bond length, and the magnitude of the d−π^* back-donation are modified similarly whether NH_3 is added explicitly or electrons are simply added to the cluster. However, the

* To whom correspondence should be addressed.

S1089-5647(98)01054-2 CCC: $15.00
Published on Web 05/07/1998

metal−CO vibration, the metal−CO bond length, and the magnitude of the s−d donation are all altered in the opposite direction. Therefore, these authors concluded that the effects of the coadsorption of NH_3 with CO cannot arise simply from electron transfer from NH_3 to CO through the metal. Other more subtle effects must also be involved.

2. Experimental Section

The experiments have been carried out in a ultrahigh-vacuum (UHV) chamber which has been described in detail previously[44] and whose base pressure was $<1 \times 10^{-10}$ Torr. Briefly, the UHV chamber is equipped with capabilities for HREELS (LK2000), Auger electron spectroscopy (AES), LEED, and TPD. HREEL spectra were acquired with a primary energy of 3 eV and a typical resolution of 50−60 cm^{-1}. TPD measurements were made with the QMS in line-of-sight with the sample and with a linear heating rate of ∼5 K/s. To avoid electron beam damage, the sample was biased at −100 V during the TPD experiments. The sample could be resistively heated to 1500 K or heated to 2200 K using an electron beam assembly. The sample temperature was measured using a W−5% Re/W−26% Re thermocouple spot-welded to the sample's edge. The Mo(110) crystal was cleaned by annealing in 2×10^{-8} Torr of O_2 at 1200 K, with a subsequent flash to 2000 K. This procedure was repeated several times until no contaminations could be detected via AES.

The palladium source used for deposition was a 0.25 mm Pd wire (99.997%, Johnson Matthey Chemical Limited) wrapped around a tungsten filament. A line-of-sight mass spectrometer was used to monitor the Pd flux which typically corresponded to approximately one monolayer (ML) per minute. The Pd source has been extensively outgassed before use; the pressure during evaporation never exceeded 3×10^{-10} Torr. The Pd coverage was calibrated using TPD and AES. The growth and annealing behavior of Pd on Mo(110) was studied by Park et al.,[45] using AES, XPS, LEED, and the change in work function. At monolayer or less coverage, Pd forms a pseudomorphic monolayer with no indication of alloy formation. At higher coverages, Pd grows in a layer-by-layer or Frank−van der Merwe mode at room temperature. At elevated temperatures, Pd grows layer-by-layer in the first layer followed by three-dimensional (3D) clustering or a Stranski−Krastanow mechanism. Annealing the Mo(110) surface exposed to Pd vapor at room temperature to 600 K will also cause the Pd multilayer to agglomerate. Significant alloying of Pd with Mo via diffusion of Mo into Pd occurs; however, even with the alloying, the surface is still covered by a monolayer of Pd. If the Pd multilayer grown at room temperature exceeds 12 ML, annealing to temperatures as high as 900 K will not cause coalescence, apparently due to kinetic considerations. The thick Pd layer shows a sharp hexagonal LEED pattern, indicating epitaxial growth and the formation of a Pd(111) overlayer structure. Only monolayer palladium and multilayer (>15 ML) Pd structures with sharp LEED patterns have been utilized in the present studies. For brevity, the Pd monolayer on Mo(110) and the epitaxially grown Pd multilayer on Mo(110) will be referred to as the Pd_{1ML}/Mo(110) and Pd(111)/Mo(110) surfaces in the following sections.

The ammonia (Matheson, 99.99%) was used after several freeze−pump−thaw cycles in the gas manifold. Carbon monoxide (Matheson, 99.99%) was used as received without further purification. The gases were introduced via a directional gas doser to the surface for TPD measurements, while the exposures for the HREELS experiments were carried out via backfilling the UHV chamber. The exposures are given in langmuirs, equal to 1×10^{-6} Torr·s, without correction for the dose enhancement and ion gauge sensitivity. For low coverages, the exposures have been converted in certain cases to coverage using LEED and HREELS results and assuming a constant sticking coefficient.

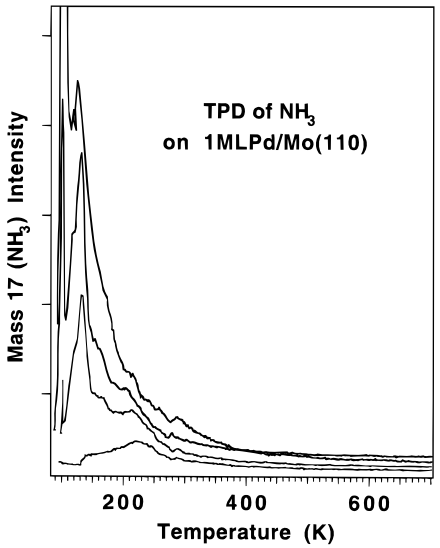

Figure 1. 1. TPD spectra of NH_3 from the Pd_{1ML}/Mo(110) surface at various NH_3 exposures.

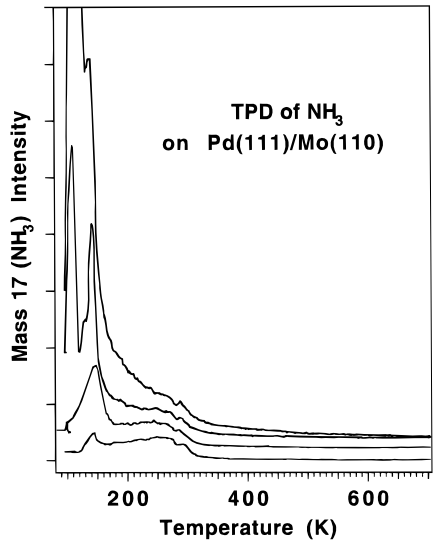

Figure 2. 2. TPD spectra of NH_3 from the Pd(111)/Mo(110) surface at various NH_3 exposures.

3. Results

3.1. NH_3 Adsorption. *3.1.1. LEED and TPD.* The adsorption of NH_3 was first studied using TPD with masses 2, 17, 18, 28, and 32 routinely monitored. On both Pd_{1ML}/Mo(110) and Pd(111)/Mo(110) surfaces, molecular NH_3 desorption is the only product found in the gas phase. Consistently, AES after TPD experiments showed a surface free of nitrogen, indicating that NH_3 adsorbs molecularly and that the adsorption is completely reversible. Figures 1 and 2 show two series of TPD spectra acquired after increasing exposures of NH_3 to Pd_{1ML}/Mo(110) and Pd(111)/Mo(110) surfaces, respectively. The TPD spectra of Figure 1 for the Pd_{1ML}/Mo(110) surface show desorption features between 140 and 350 K for low exposures of NH_3. Three broad and significantly overlapping peaks centered at 160,

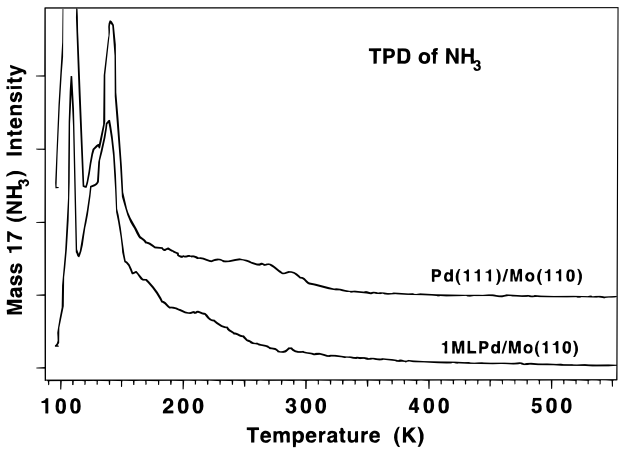

Figure 3. 3. Comparison of TPD spectra on the Pd_{1ML}/Mo(110) surface with the Pd(111)/Mo(110) surface at a NH_3 coverage of approximate 1.5 ML.

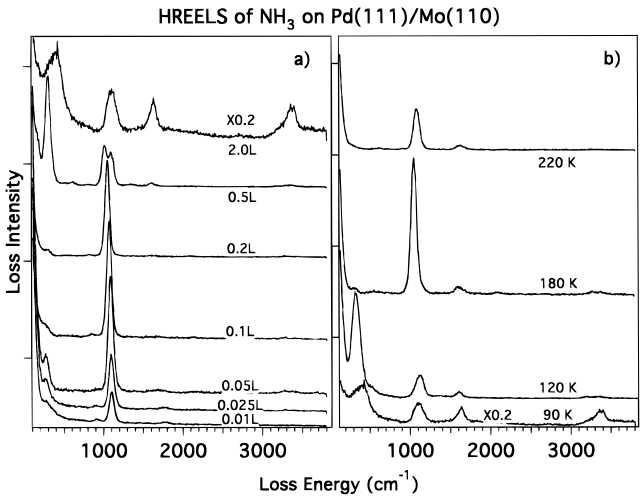

Figure 4. 4. HREEL spectra of NH_3 on the Pd(111)/Mo(110) surface: (a) after increasing exposures, (b) after dosing ca. 4 ML of NH_3 at 90 K and subsequently annealing to the indicated temperature.

225, and 280 K are apparent. With increasing NH_3 exposures, the features between 150 and 350 K become more intense, and two new features at 100 and 130 K begin to develop. The feature at 100 K does not saturate but shifts gradually to higher desorption temperatures with increasing NH_3 dose. This feature is assigned to desorption of NH_3 from the multilayer. The feature at 130 K, with a desorption temperature between the multilayer and the first chemisorbed layer, is assigned to second-layer desorption. The Pd(111)/Mo(110) surface displays very similar TPD behavior as shown in Figure 2. Two desorption features between 90 and 150 K are observed, again attributed to desorption from the condensed and second layers, respectively. The chemisorbed layer, however, shows a slightly larger proportion of the high-temperature desorption state on the Pd(111)/Mo(110) surface compared to the Pd_{1ML}/Mo(110) surface. This is more evident in Figure 3, where TPD spectra from the two surfaces are compared. From Figure 3 one can conclude that a significant fraction of the desorption feature near 270 K on the Pd(111)/Mo(110) surface is shifted to a lower desorption temperature on the Pd_{1ML}/Mo(110) surface. However, the high-temperature state near 270 K is still populated on the Pd_{1ML}/Mo(110) surface, but with reduced intensity.

The adsorption of NH_3 on these two surfaces has been further studied with LEED. On the Pd(111)/Mo(110) surface, no additional LEED spots were observed upon NH_3 exposures and subsequent annealing. In contrast, the Pd_{1ML}/Mo(110) surface exhibited a (2×2) LEED pattern after annealing to 180 K after dosing with approximately 3 ML of NH_3. This temperature is sufficient to remove both multilayer and second-layer ammonia, leaving a surface covered with only a chemisorbed layer of ammonia. The LEED pattern is very sensitive to the electron beam and can be observed only for a relatively short time period, indicating a high cross section of electron-induced desorption for NH_3 on the Pd_{1ML}/Mo(110) surface. This is consistent with the relative weak bonding of NH_3 on this surface. The (2×2) LEED pattern observed here has been previously observed by Benndorf and Madey[46] for NH_3 on the Ru(001) surface but could not be confirmed by Sasaki et al.[40]

3.1.2. HREELS. Figure 4a shows a series of HREEL spectra acquired subsequent to increasing NH_3 exposures on the Pd(111)/Mo(110) surface. At an exposure of 0.01 langmuir, two features are seen at 290 and 1100 cm^{-1}, which can be assigned to the Pd−N stretching and symmetric deformation (umbrella) modes of adsorbed NH_3, respectively. No features related to the N−H stretching were observed, presumably due to the low cross section for these modes. Upon increasing the NH_3 exposure from 0.01 langmuir, the features at 290 and 1100 cm^{-1} gain intensity until 0.05 langmuir is reached; the 290 cm^{-1} feature then loses intensity with a further increase in exposure to 0.2 langmuir. Concomitantly, a new feature at 300 cm^{-1} begins to appear at 0.2 langmuir. The intensity of the peak at 1100 cm^{-1} is almost constant between 0.05 and 0.1 langmuir and then begins to attenuate with exposures up to 0.2 langmuir. The symmetric deformation mode gradually shifts from 1100 to 1050 cm^{-1} with increasing NH_3 exposures from 0.01 to 0.2 langmuir. At an exposure of 0.025 langmuir, features between 3200 and 3500 cm^{-1}, assigned to N−H stretching modes, begin to develop. With increasing NH_3 exposure from 0.2 to 0.5 langmuir, the feature at 1050 cm^{-1} shifts further to 1005 cm^{-1} and dramatically loses intensity. Concomitantly, two new features appear at 1100 and 1610 cm^{-1}, while the feature at 300 cm^{-1} dominates at this coverage. These features collectively can be assigned to bilayer formation. The peaks at 300 and 1610 cm^{-1} correspond to the NH_3 twisting mode and the asymmetric deformation mode, respectively. The NH_3 twisting mode is very characteristic of second-layer ammonia on various surfaces and has been used as a fingerprint for the onset of second-layer ammonia adsorption.[20] This mode is not visible in the first chemisorbed layer due to free rotation about the N−metal bond.[46] In the second ammonia layer, the formation of hydrogen bonds between the ammonias hinders this rotation considerably and shifts its frequency to an accessible frequency in the HREELS measurements. The top spectrum of Figure 4a is that acquired after dosing 2 langmuirs of NH_3 (approximately 5−6 monolayers). In this spectrum, features at 420, 1100, and 1625 cm^{-1} and a doublet at 3360 and 3400 cm^{-1} are apparent. These features correlate with the formation of the NH_3 multilayer phase and can be assigned to the frustrated libration (twisting mode), the symmetric and asymmetric deformation, and the symmetric and asymmetric stretching vibrational modes, respectively.

In Figure 4b, an annealing series after dosing approximately four NH_3 layers on the Pd(111)/Mo(110) surface at 90 K is shown. After heating to 120 K to remove the multilayer, the spectrum characteristic of the bilayer is seen, with dominating features at 320 cm^{-1} due to the NH_3 twisting mode and the symmetric and asymmetric deformation mode at 1120 and 1600 cm^{-1}, respectively. Further annealing to 180 K desorbs the second layer with the subsequent spectrum being dominated by the symmetric deformation at 1050 cm^{-1}. Also seen are the

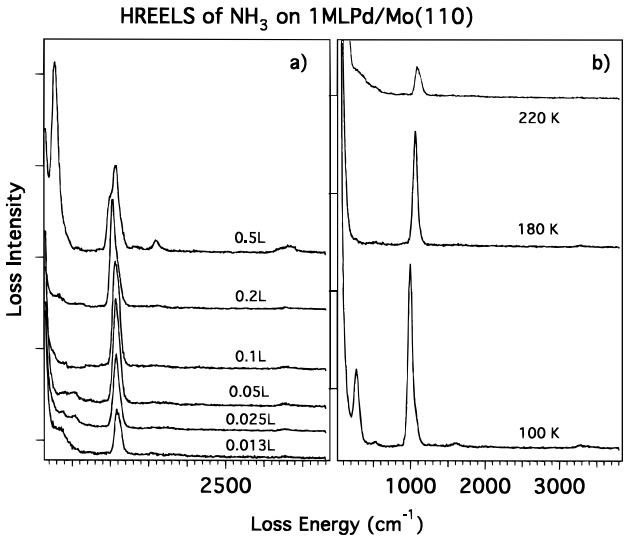

Figure 5. 5. HREEL spectra of NH_3 on the Pd_{1ML}/Mo(110) surface: (a) after increasing exposures, (b) after dosing about 4 ML of NH_3 at 90 K and subsequently annealing to the indicated temperature.

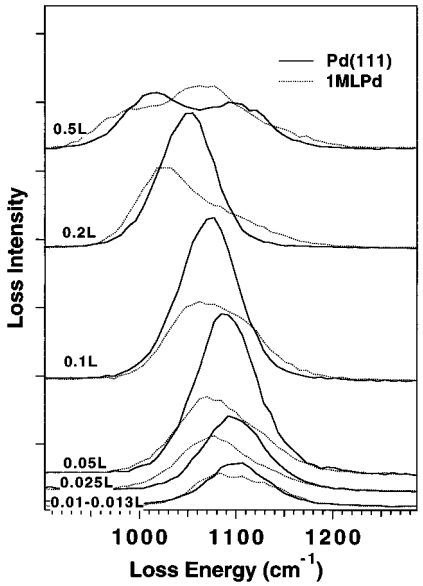

Figure 6. 6. Comparison of the NH_3 symmetric deformational mode on the Pd_{1ML}/Mo(110) surface with the Pd(111)/Mo(110) surface at various NH_3 coverages.

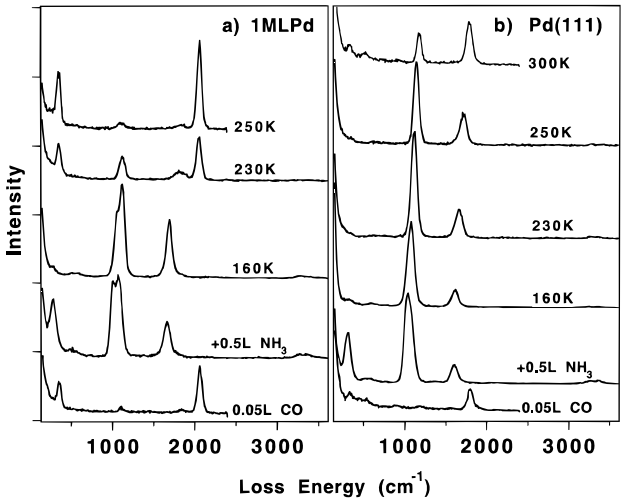

Figure 7. 7. HREEL spectra after dosing 0.5 langmuir of NH_3 with 0.05 langmuir of CO precovered on (a) Pd_{1ML}/Mo(110) and (b) Pd(111)/Mo(110) surfaces and subsequently annealing to the indicated temperature.

Pd−N vibrational mode at 300 cm^{-1} and the asymmetric and symmetric N−H stretching modes at 3260 and 3365 cm^{-1}, respectively. A small feature at 1600 cm^{-1} is also apparent, which is most likely due to a trace amount of coadsorbed CO. This feature is less likely due to the asymmetric deformation of NH_3, since the asymmetric deformation mode is not observed at a similar coverage in the coverage series of Figure 4a, whereas CO coadsorbed with NH_3 shows a C−O vibrational mode at this frequency (see below). Upon heating the sample to even higher temperatures, the feature at 1050 cm^{-1} loses intensity and shifts to a higher wavenumber due to desorption of NH_3 from the chemisorbed first layer.

A palladium monolayer supported on Mo(110), Pd_{1ML}/Mo(110), exhibits HREELS spectra analogous to those of the Pd(111)/Mo(110). This can be seen in Figure 5a,b. In Figure 5a, the HREELS spectra acquired after increasing NH_3 exposures are shown, while Figure 5b shows an annealing series. As for Pd(111)/Mo(110), the symmetric NH_3 deformation, which gradually gains intensity and shifts to lower wavenumber with increasing NH_3 coverage, is the dominating feature up to a NH_3 exposure of 0.2 langmuir. The intensity of this feature decreases with further increasing exposure to 0.5 langmuir. The features correlated to the bilayer NH_3 dominate the spectrum at 0.5 langmuir. However, careful inspection of the symmetric deformation shows some differences on the two surfaces that are more evident in Figure 6. On the Pd_{1ML}/Mo(110) surface, the features are generally broad and shift more rapidly to lower wavenumbers with increasing NH_3 exposures. The intensity change with increasing NH_3 is more profound for the Pd(111)/Mo(110) surface than the Pd_{1ML}/Mo(110) surface. Also, an asymmetric peak shape is apparent for the Pd_{1ML}/Mo(110) surface.

3.2. Coadsorption of NH_3 with CO. The influence of NH_3 on the vibrational structure of coadsorbed CO on the Pd_{1ML}/Mo(110) and Pd(111)/Mo(110) surface has been studied using HREELS over a wide coverage range. In the following sections these results are described and the two surfaces compared at various coverages.

3.2.1. 0.05 langmuir of CO + 0.5 langmuir of NH_3. Figure 7 shows HREEL spectra for the Pd_{1ML}/Mo(110) (left) and Pd(111)/Mo(110) (right) systems at a relatively small CO and a relatively large NH_3 coverage. From bottom to top, the spectra acquired after dosing 0.05 langmuir of CO, then 0.5 langmuir of NH_3, and finally an anneal to the indicated temperature are shown. The spectra taken for a 0.05 langmuir CO exposure show features at 350 and 2050 cm^{-1} on the Pd_{1ML}/Mo(110) surface and features at 320 and 1800 cm^{-1} on the Pd(111)/Mo(110) surface. These can be assigned to CO adsorption on the atop and 3-fold hollow sites, respectively. Dosing 0.5 langmuir of NH_3 on top of these surfaces induces a dramatic red shift of the C−O stretching vibration by 400 cm^{-1} for Pd_{1ML}/Mo(110) and 200 cm^{-1} for Pd(111)/Mo(110). Concomitantly, the features due to the Pd−CO stretching mode are replaced by the NH_3 twisting mode arising from NH_3 in the second layer. The NH_3 symmetric deformational mode exhibits a doublet at 1010 and 1080 cm^{-1} for Pd_{1ML}/Mo(110) and a single, broad peak at 1030 cm^{-1} for Pd(111)/Mo(110). Also, the asymmetric and symmetric N−H stretching modes are clearly seen for both surfaces. Since the NH_3 desorbs at a lower temperature than CO, the coadsorption of NH_3 at relatively low coverages with the same CO surface coverage has been studied by annealing the surface to the indicated temperature in Figure 7. The surface

was first annealed to 160 K to remove the NH_3 second layer, and as anticipated the peak near 300 cm^{-1} essentially disappears. Only a small feature, likely relating to the Pd−N stretching mode, remains near 300 cm^{-1}. It should be noted that the Pd−CO stretching mode is not observed for either surface, although this mode has a very high intensity on the NH_3-free Pd_{1ML}/Mo(110) surface. A small shift (10−15 cm^{-1}) in both the NH_3 symmetric deformational mode and the CO stretching vibrational mode to higher wavenumber is also apparent in this temperature range. On the Pd_{1ML}/Mo(110) surface, the doublet near 1050 cm^{-1} is replaced by a feature at 1010 cm^{-1} with a shoulder on the low wavenumber side. The HREEL spectra of NH_3 alone on the Pd_{1ML}/Mo(110) and Pd(111)/Mo(110) surfaces show a NH_3 symmetrical, deformational mode for the first chemisorbed layer below 1005 cm^{-1} and, for the second layer, a feature between 1065 and 1100 cm^{-1} at 0.5 langmuir of NH_3. Comparing the results of coadsorbed NH_3 and CO with NH_3 alone, it is apparent that the presence of CO on the surface shifts the NH_3 symmetrical deformational mode for the first chemisorbed layer of NH_3 to a higher frequency. For the Pd(111)/Mo(110) surface, this shift causes the feature for the first chemisorbed layer to collapse into the feature for the second adsorbed layer, resulting in a single NH_3 symmetric deformation peak.

To further reduce the NH_3 coverage, the sample was heated from 160 to 300 K, and HREEL spectra were acquired after anneals to 230, 250, and 300 K. In this temperature range, the NH_3 symmetric deformation and the C−O stretching vibration gradually shift to higher wavenumbers on the Pd(111)/Mo(110) surface. For the Pd_{1ML}/Mo(110) surface the C−O stretching mode moves to 2050 cm^{-1} with a small feature at 1800 cm^{-1} becoming apparent at 230 K. Also seen is the reappearance of the Pd−CO stretching mode at 350 cm^{-1} for the Pd_{1ML}/Mo(110) surface. The disappearance and reappearance of this peak correlate with the absence and presence of CO adsorbed on the atop site. The coadsorption of NH_3 shifts the CO adsorption from the atop site to the three-hollow site. The Pd−CO vibrational mode of CO adsorbed on the three-hollow site apparently has a smaller intensity and lower vibrational frequency than does CO adsorbed on the atop site and is obscured by the NH_3 twisting mode.

On the Pd_{1ML}/Mo(110) surface, the features related to NH_3 are greatly reduced upon heating to 250 K after which the C−O stretching mode moves to its position prior to the dosing of NH_3. Also, the peak desorption temperature of NH_3 is much higher for the Pd(111) surface. Even at 300 K, significant amounts of NH_3 remain on the surface, as indicated by the feature at 1170 cm^{-1}. These results show a higher binding energy for NH_3 on the Pd(111)/Mo(110) surface than for the Pd_{1ML}/Mo(110) surface, even in the presence of CO. Furthermore, by comparing the anneal series with coadsorbed NH_3 to that acquired on the CO-free surface, it can concluded that coadsorption of NH_3 with CO increases the NH_3 binding energy. This conclusion is also valid for other CO coverages, as discussed below.

3.2.2. 0.25 langmuir of CO + 0.5 langmuir of NH_3. Figure 8 shows two series of HREEL spectra acquired after dosing 0.5 langmuir of NH_3 to the Pd_{1ML}/Mo(110) and Pd(111)/Mo(110) surfaces, precovered with 0.25 langmuir of CO, and a subsequent anneal of each to the indicated temperature. For reference, the spectra of the surfaces with only CO are shown at the bottom. The peaks at 360 and 2060 cm^{-1} on the Pd_{1ML}/Mo(110) and at 320 and 1830 cm^{-1} on the Pd(111)/Mo(110) surface can be assigned to the Pd−CO and C−O stretching modes, respectively. The adsorption sites are atop for the Pd_{1ML}/Mo(110) surface and likely three-hollow for the Pd(111)/Mo(110) surface. Dosing 0.5 langmuir of NH_3 on top of these surfaces shifts the C−O stretching vibration to lower wavenumber. On the Pd_{1ML}/Mo(110) surface, two features corresponding to C−O stretching modes appear at 1705 and 1810 cm^{-1}, while on the Pd(111)/Mo(110) surface a feature at 1750 cm^{-1} with a shoulder at 1600 cm^{-1} is seen. As for lower CO coverages, the features corresponding to the Pd−CO stretching modes are not observed. Instead, the NH_3 twisting modes are observed in this frequency range. It is noteworthy that this twisting mode is much weaker for the Pd_{1ML}/Mo(110) surface compared to the Pd(111)/Mo(110) surface or to the Pd_{1ML}/Mo(110) surface with a lower CO coverage. This is probably due to the lower capacity of the Pd_{1ML}/Mo(110) surface for the adsorption of CO and NH_3. At an exposure of 0.25 langmuir of CO, the amount of NH_3 adsorbed in the first chemisorbed layer on the Pd_{1ML}/Mo(110) is smaller than on the Pd(111)/Mo(110) surface. The bilayer structure for Pd_{1ML}/Mo(110) is therefore limited to a relatively small part of the surface, suggesting that the twisting mode at 300 cm^{-1} is characteristic of NH_3 on top of NH_3. This is consistent with the observation that hydrogen bonding shifts this vibrational feature to an accessible value for detection by HREELS.

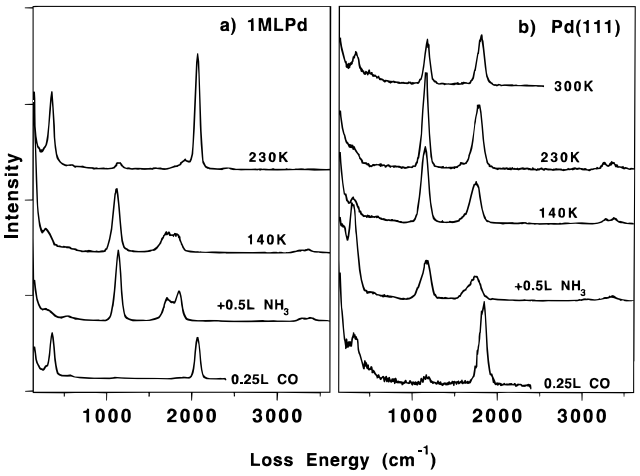

Figure 8. 8. HREEL spectra after dosing 0.5 langmuir of NH_3 with 0.25 langmuir of CO-precovered (a) Pd_{1ML}/Mo(110) and (b) Pd(111)/Mo(110) surfaces and subsequently annealing to the indicated temperature.

To examine the effect of NH_3 coverage on CO adsorption at 0.5 langmuir, both surfaces were gradually annealed to 300 K. Following the desorption of the second NH_3 layer by annealing to 140 K, the features corresponding to the NH_3 twisting mode lose intensity. The NH_3 symmetric deformational mode and the C−O stretching mode also show changes in the line shape without a significant shifting of the primary features. No significant shifts were observed for the NH_3 symmetric deformational mode even at the higher annealing temperatures. However, the C−O stretching mode shifts from 1750 to 1800 cm^{-1} for the Pd(111)/Mo(110) surface and from 1705 or 1810 $^-$ to 2060 cm^{-1} on the Pd_{1ML}/Mo(110) surface. A small feature at 1910 cm^{-1} is also seen on the Pd_{1ML}/Mo(110) surface after annealing the surface to 230 K, which is probably due to CO interacting with small amounts of NH_3 remaining on the surface. After desorbing essentially all of the NH_3, the Pd−CO stretching mode regains its original intensity.

3.2.3. 0.5 langmuir of CO + 0.5 langmuir of NH_3. The most striking finding in this coverage range, as shown in Figure 9, is the C−O stretching mode at 1850 cm^{-1} for Pd_{1ML}/Mo(110) and at 1780 cm^{-1} for Pd(111)/Mo(110). Each of these features

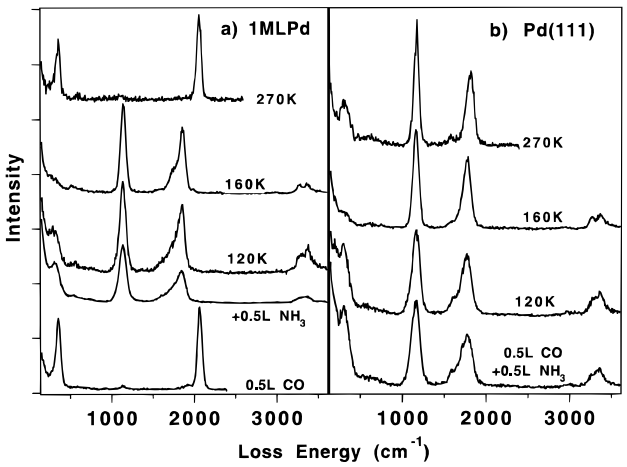

Figure 9. 9. HREEL spectra after dosing 0.5 langmuir of NH_3 onto 0.5 langmuir of CO-precovered (a) Pd_{1ML}/Mo(110) and (b) Pd(111)/Mo(110) surfaces and subsequently annealing to the indicated temperature.

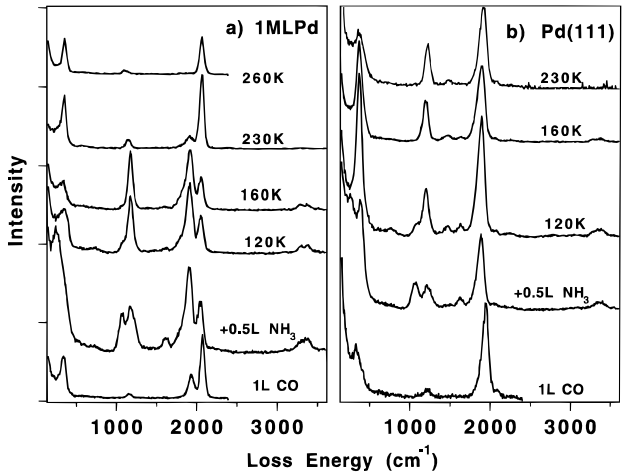

Figure 10. 10. HREEL spectra after dosing 0.5 langmuir of NH_3 onto 1.0 langmuir of CO-precovered (a) Pd_{1ML}/Mo(110) and (b) Pd(111)/Mo(110) surfaces and subsequently annealing to the indicated temperature.

exhibits a foot extending with gradually decreasing intensity to 1500 cm^{-1}. These results suggest a long-range interaction between coadsorbed CO and NH_3 on both surfaces. Also noteworthy is that the main C−O stretching feature does not shift with annealing temperature to 160 K and that the NH_3 symmetric deformational mode does not shift during the entire annealing cycle of these experiments.

As for lower CO coverages, the Pd−CO vibrational mode is quenched in the presence of NH_3, with the NH_3 twisting mode becoming apparent. The N−H stretching mode is also observed with a relatively high intensity.

3.2.4. High (1.0 langmuir) CO Coverage and 0.5 langmuir of NH_3. The influence of NH_3 on CO coadsorption at high CO coverage is shown in the HREEL spectra of Figure 10. The spectra of CO on the NH_3-free surfaces correspond to CO adsorption on the bridging site of Pd(111)/Mo(110) and both bridging and atop sites on Pd_{1ML}/Mo(110). Dosing 0.5 langmuir of NH_3 on top of the CO-precovered surface causes again rather dramatic changes in the C−O and Pd−CO vibrational regions.

For the Pd_{1ML}/Mo(110) surface, the intensity of the C−O vibrational mode shifts from a feature corresponding to the atop site to a feature related to the bridging site, with a small shift of both features to lower wavenumber. The peak at 1905 cm^{-1} shows as before a foot with decreasing intensity extending to lower wavenumber. The feature at 330 cm^{-1} corresponding to the Pd−CO stretching mode disappears into the shoulder of the feature corresponding to the NH_3 twisting mode. Two well-separated features related to the NH_3 symmetric deformational modes are observed at 1080 and 1180 cm^{-1}. In contrast to the spectra acquired at lower CO coverages, a feature due to the NH_3 asymmetric deformational mode is apparent at 1610 cm^{-1}. Upon heating to 120 K, the feature at 250 cm^{-1} disappears and the Pd−CO vibration at 350 cm^{-1} regains some of the intensity; the latter's intensity is completely restored by heating to 230 K. The feature at 1080 cm^{-1} loses significant intensity upon heating to 120 K and then disappears completely at 160 K with desorption of the NH_3 second layer. This indicates that the large blue shift of the NH_3 symmetric deformational mode is due to a surface-mediated interaction rather than a direct through-space interaction between CO and NH_3. Otherwise, one would expect to see a large shift as well for NH_3 adsorbed in the second layer. It should be noted that the NH_3 symmetric deformational mode for the first chemisorbed layer is at a higher wavenumber than that for the second layer. This result contrasts with that for the surfaces covered with only NH_3, where the first chemisorbed layer displays a lower vibrational frequency for the NH_3 symmetric deformational mode (between 970 and 1010 cm^{-1}) than the second adsorbed NH_3 layer (between 1065 and 1100 cm^{-1}). The gradual shift of the NH_3 symmetric deformational mode to higher wavenumber with increasing CO coverages is the result of two processes. First, the presence of CO on the surface reduces the NH_3 density in the first layer, therefore reducing the NH_3−NH_3 repulsive interaction. Second, the attractive interaction between NH_3 and CO shifts the NH_3 symmetric deformational mode to a higher frequency. Since the NH_3 symmetric deformation shows a vibrational frequency of approximately 1100 cm^{-1} at the zero-coverage limit with no CO coadsorbate, well below the vibrational frequency (1180 cm^{-1}) with coadsorbed CO, the shift induced by the NH_3−CO attractive interaction contributes most significantly to the observed shift in the frequency of the NH_3 symmetric deformation.

Coadsorption of CO with NH_3 slightly shifts the C−O stretching vibration to lower frequency from 1940 to 1890 cm^{-1}. Two NH_3 symmetric deformation features are observed at 1160 and 1210 cm^{-1}, with the lower frequency feature disappearing after annealing to 160 K. Both the Pd−CO and the NH_3 twisting vibrational modes are evident. A new feature at 1480 cm^{-1}, which was not observed at lower CO coverages, is apparent and becomes more evident upon annealing the surface to 120 K. This feature is still evident even after heating the sample to 230 K. This feature obviously arises from the relatively high coverage of CO. To confirm this, HREEL spectra were acquired after dosing 0.5 langmuir of NH_3 onto a 3 langmuirs CO-precovered Pd(111)/Mo(110) surface. The resulting HREEL spectra are shown in Figure 11. As anticipated, the feature at 1490 cm^{-1} is now even more intense. The low frequency of this feature precludes a CO-related origin. This peak is assigned accordingly to the asymmetric deformation of NH_3. The high intensity of this peak suggests that NH_3 is no longer present in an upright configuration.

3.2.5. NH_3 + CO. The effect of CO on coadsorbed NH_3 can be more clearly seen if one doses CO onto an NH_3-precovered surface. HREEL spectra acquired after dosing 0.5 langmuir of CO on a 0.4 langmuir NH_3-precovered surface are shown in Figure 12. Spectra for NH_3 alone are shown at the bottom of (a) and (b). Each surface was covered slightly in access of 1 ML of NH_3, as indicated by the feature at 300 cm^{-1} and the

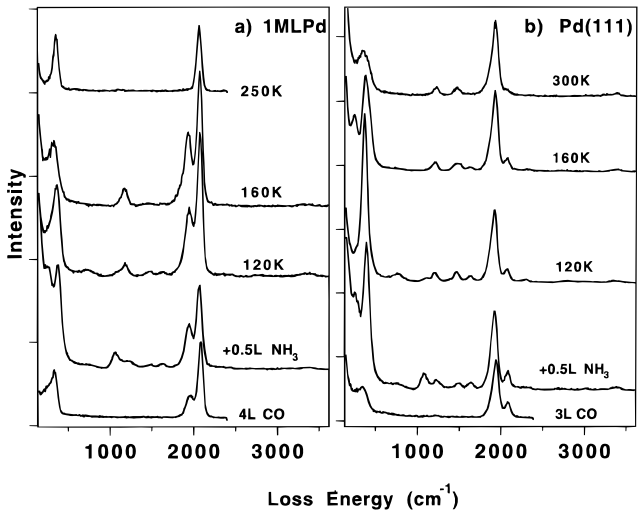

Figure 11. 11. HREEL spectra after dosing 0.5 langmuir of NH_3 onto 4.0 langmuir of CO-precovered (a) Pd_{1ML}/Mo(110) and (b) Pd(111)/Mo(110) surfaces and subsequently annealing to the indicated temperature.

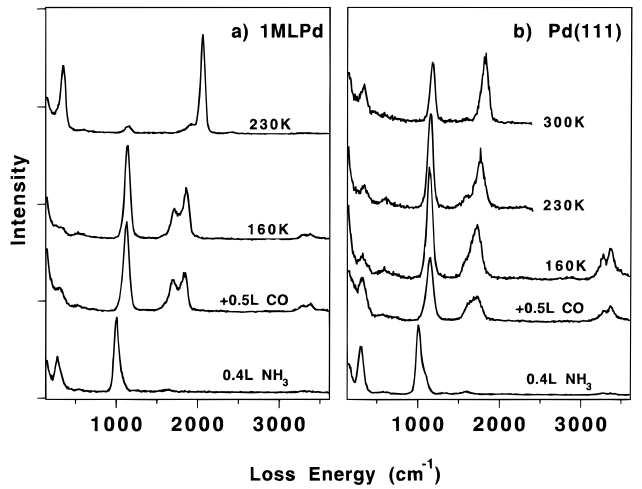

Figure 12. 12. HREEL spectra after dosing 0.5 langmuir of CO onto 0.4 langmuir of NH_3-precovered (a) Pd_{1ML}/Mo(110) and (b) Pd(111)/Mo(110) surfaces and subsequently annealing to the indicated temperature.

small shoulder at 1100 cm^{-1}. Coadsorption with CO shifts the feature at 1000 cm^{-1} to 1140 cm^{-1}. The feature at 300 cm^{-1} loses some intensity, likely to displacement of NH_3 in the chemisorbed layer by CO. The intensity of the N−H stretching vibrations, however, is enhanced by the present of CO. Two peaks corresponding to C−O stretching modes are seen at 1700 and 1850 cm^{-1} for Pd_{1ML}/Mo(110) and at 1610 and 1720 cm^{-1} for Pd(111)/Mo(110). Upon annealing, the NH_3 symmetric deformational mode loses intensity without shifting significantly, while the C−O stretching modes gradually shift to higher wavenumber.

3.2.6. 0.02 langmuir of CO + 0.02 langmuir of NH_3. The interaction of CO and NH_3 at the zero-coverage limit has also been studied after dosing 0.02 langmuir of CO and 0.02 langmuir of NH_3 on Pd_{1ML}/Mo(110), corresponding to less than 10% of the saturation coverage for each species. The HREELS results are shown in Figure 13. From bottom to top, the surface has been annealed to higher temperatures as indicated. At 90 K, features at 345, 1105, 1750, 1850, and 2010 cm^{-1} are apparent and can be attributed to the Pd−CO vibration, the NH_3 deformation, and the CO stretching mode for the three-hollow,

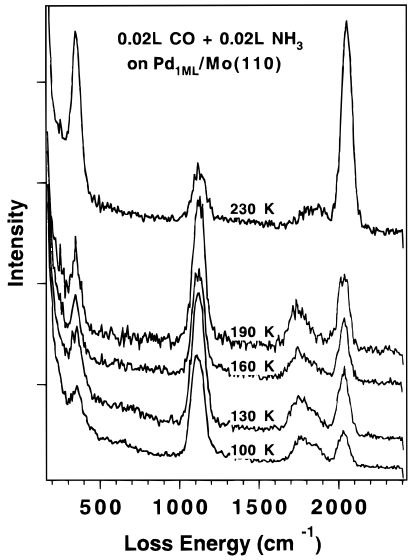

Figure 13. 13. HREEL spectra after dosing 0.02 langmuir of CO onto 0.02 langmuir of NH_3 precovered on Pd_{1ML}/Mo(110) and subsequently annealing to the indicated temperature.

the 2-fold bridging, and the atop site, respectively. Annealing to 230 K leads to a dramatic decrease in the NH_3 deformation mode and an intensity transfer from the feature at 1750 cm^{-1} to that at 2010 cm^{-1}, indicating desorption of NH_3 and a change of CO from the 3-fold hollow to the atop site. This evidence of significant interaction at such small coverages indicates the formation of mixed chemisorbed layers of CO and NH_3. This is consistent with an attractive interaction between CO and NH_3 and repulsive CO−CO and NH_3−NH_3 interactions.

4. Discussion

4.1. NH_3 Adsorption. The adsorption of NH_3 has been previously studied on various surfaces using TPD.[19−34] Consistent with these previous results, the TPD spectra of NH_3 in the present study show a broad desorption peak for the chemisorbed state on both the Pd_{1ML}/Mo(110) and Pd(111)/Mo(110) surfaces. This is due to the increasing repulsive interaction between the adsorbed NH_3 with increasing coverage. NH_3 adsorbs via a dative bond through the electron lone pair on the N atom, leading to a relatively large dipole between NH_3 and the surface. These dipoles interact repulsively with each other, therefore destabilizing the NH_3. This general picture is consistent with work function measurements of NH_3 adsorbed on Ru(001) by Benndorf and Madey.[46] These authors found that the work function initially decreases linearly with increasing NH_3 coverage due to electron donation from NH_3 to the surface but then decreases less rapidly up 0.15 ML due to depolarization. The other possible explanation for the broad desorption feature observed for chemisorbed NH_3 is the presence of multiple adsorption sites.[23,32] However, the single narrow feature observed for the NH_3 symmetric deformational mode for the chemisorbed NH_3 layer on Pd(111)/Mo(110) indicates that this is unlikely. In this context it is noteworthy that, in the IR measurements of NH_3 adsorption on Ru(0001) by Rodriguez et al.,[19] only a single feature for chemisorbed NH_3 is observed.

The adsorption of NH_3 is completely reversible for both Pd_{1ML}/Mo(110) and Pd(111)/Mo(110); no indication of dissociation is found in the TPD and HREELS data. The adsorption of NH_3 on several of the later transition metals has also been found previously to be largely reversible. These include Ru(001), Pt(111), Ni(111), and Ni(110). Only on Ni-

(110) has a substantial amount of dissociation been found after dosing NH_3 at room temperature.[44]

HREELS has been used to study NH_3 adsorption on Ru(001), Pt(111), Ni(111), Ni(110), Ag(110), Ag(311), and Fe(110). The HREEL spectra of chemisorbed NH_3 in most of these cases are dominated by the NH_3 asymmetric deformational mode. The wavenumber of this vibrational feature has been correlated either to the strength of the NH_3−metal bond[39] or to the charge density at the substrate atoms.[20] NH_3 adsorbed on NiO(100) shows a very similar TPD spectra as for the transition metal; however, no shift in the NH_3 asymmetric deformational mode with increasing NH_3 coverage is apparent. This is likely due to the localized nature of the charge in an insulating oxide. Thus, the shift of the symmetric deformational mode with increasing NH_3 coverage is likely dominated by effects related to the electron density at the surface. In any event, this shift is a measure of the ability of the substrate to accept and stabilize the nitrogen electron lone pair of NH_3. This, in turn, correlates to the density of states near the Fermi level as well as the electron density within individual orbitals. That this vibration has exactly the same frequency for both Pd_{1ML}/Mo(110) and Pd(111)/Mo(110) surfaces at lower NH_3 coverage and decreases to lower frequency at a more rapid rate on the Pd_{1ML}/Mo(110) surface than on the Pd(111)/Mo(110) surface indicates a slightly enhanced reduction in the density of states near the Fermi level for the Pd_{1ML}/Mo(110) surface compared to Pd(111)/Mo(110), but a very similar electron density of individual orbitals for both systems. In this respect a slightly reduced high-temperature state in TPD for NH_3 adsorbed on Pd_{1ML}/Mo(110) in comparison to the Pd(111)/Mo(110) surface has been found.

Previously, a reduced binding energy has been found for CO bound to a Pd monolayer on a number of substrates, including transition metals, noble metals, and sp metals such as Al. This indicates that the reduced reactivity of monolayer Pd is an intrinsic property. An interaction with the substrate will certainly further modify the electronic structure of the Pd monolayer, which accounts for the differences in Pd monolayers supported on various substrates since the CO reduced binding energy has been attributed primarily to reduced back-bonding from the metal. In this study, the reduced ability of a Pd monolayer to accept electrons has been demonstrated and is clearly due to a reduced density of states near the Fermi level. The monolayer presents a transition from an atomiclike structure with discrete states to a band structure with continuous states. Angular-resolved ultraviolet photoemission spectroscopy (ARUPS) of monolayer Pd on Al(111), where the features corresponding to the Pd monolayer can be clearly distinguished from the substrate emission, shows that the transition from the atomiclike structure is not yet complete at a monolayer coverage of Pd. That is, an atomiclike electronic structure in a Pd monolayer is retained to a degree. Consequently, the density of states near the Fermi level for the monolayer is less than bulk Pd, and the monolayer shows reduced reactivity.

4.2. Coadsorption of NH_3 with CO. Coadsorption of CO and NH_3 causes a blue shift of the NH_3 symmetric deformation mode and a red shift of the C−O stretching mode for monolayer and multilayer Pd. However, each of these shifts occurs to a significantly larger extent for Pd(111)/Mo(110) than Pd_{1ML}/Mo(110). This is consistent with a higher binding energy for CO and NH_3 on Pd(111)/Mo(110) compared to Pd_{1ML}/Mo(110) and indicates that the interaction between CO and NH_3 occurs primarily through the surface.

The frequency shift to lower wavenumber of the C−O vibrational mode induced by a coadsorbed electropositive species such as ammonia or alkali metals has been a subject of intensive debate. Several mechanisms have been proposed to explain this red shift. In the chemical shift model, the coadsorption of an electron donor leads to greater surface electron density, therefore leading to an enhanced electron transfer into the $2\pi^*$ antibonding orbital of the adsorbed CO. This occurs through either depolarization in the case of a more localized electron donor such as NH_3 or electron transfer into the substrate in the case of alkali metals. The consequence of the enhanced back-bonding is that the C−O bond is weakened while the CO−surface bond is stabilized. Concomitantly, the C−O stretching mode shifts to lower wavenumber. An increased binding energy of CO is also observed with the coadsorption of alkali metals. Since NH_3 desorbs well below CO from transition metals, the influence of coadsorbed NH_3 on the CO binding energy cannot be addressed using conventional TPD. However, the above arguments suggest that CO coadsorbed with NH_3 will have a higher binding energy. In contrast, the electrostatic model argues that adsorbed CO and NH_3 have opposite dipoles with respect to the surface normal. The dipole−dipole interaction then stabilizes both molecules on the surface. The blue shift is simply a result of the interaction of CO with the electrostatic field produced by the coadsorbed molecules (Stark shift).

In actuality, a combination of both charge transfer and electrostatic interaction exists. To separate these effects, Hoffman et al. studied coadsorption of CO with Xe on the Ru(001) surface.[47] Since Xe is only weakly physisorbed and charge transfer is negligible, the observed red shift of the C−O vibrational mode can be assumed to be due solely to an electrostatic interaction. Yates and co-workers[48−50] have recently studied coadsorption of CO with Xe, H_2, or O and were able to correlate the shift of the C−O vibrational mode with the global work function change. These authors argued that the shift of the C−O vibrational mode was primarily due to the alteration of the Fermi level by the coadsorbate. Depending upon the coadsorbed species, the Fermi level moves either up or down, resulting in an increase or decrease in the back-bonding and, therefore, a red or blue shift of the C−O stretching mode. The dipole−dipole interaction plays only a minor role in the observed frequency shift.

The present results for Pd_{1ML}/Mo(110) and Pd(111)/Mo(110) are consistent with both long-range and short-range interactions. The long-range interaction, likely due to a work function change, is most clearly seen at lower CO coverages on Pd(111)/Mo(110). At 0.05 langmuir CO exposure, a gradual shift of both the C−O stretching mode and the NH_3 symmetric deformation to higher frequencies with decreasing NH_3 coverage is observed. Desorbing NH_3 causes a gradual increase in the work function and therefore a decrease in the d−π^* back-bonding. The NH_3 symmetric deformational mode also shifts to higher frequency due to an attenuated NH_3−NH_3 interaction. This result can also be rationalized in terms of the work function change, which enhances the ability of the substrate to accept electrons from NH_3, thus forming a more stable bond. In any event, it is clearly a long-range, rather than a short-range, effect. On the Pd_{1ML}/Mo(110) surface, the interaction between NH_3 and CO also results in a change in the adsorption site at relatively high annealing temperatures, from the atop site to a likely 3-fold hollow site. With respect to the 3-fold hollow site, the C−O vibrational mode gradually shifts from 1680 cm^{-1} at higher CO exposures to 1810 cm^{-1} at a CO exposure of 0.05 langmuir. This shift (130 cm^{-1}) is somewhere smaller than the corresponding shift (200 cm^{-1}) found for the 3-fold hollow site on

the Pd(111)/Mo(110) surface. This is consistent with CO and NH_3 being more strongly bonded to the Pd(111)/Mo(110) surface compared to the Pd_{1ML}/Mo(110) surface. The interaction through the substrate is also more significant.

In addition to long-range interactions, short-range interactions are also clearly evident. For instance, the dosing of NH_3 on top of a CO-covered surface converts a single C−O vibration feature to two C−O vibrational features or occasionally a broad peak with a foot extending to lower wavenumbers. These results suggest either a different number of NH_3 neighboring molecules of CO or a reduced density in the NH_3 neighbors. This short-range effect is probably dominated by local charge transfer and, to a lesser degree, dipole−dipole interactions. In a charge-transfer mechanism, NH_3 donates electron density via the nitrogen atom to the substrate, polarizing the substrate electron density such that the d−π back-donation is increased.

It is also noteworthy that the presence of NH_3 promotes the occupancy by CO of more highly coordinated sites on the surface, with the Pd monolayer appearing more bulklike with respect to CO adsorption. It has been demonstrated[18] that CO bonded to a 3-fold hollow site is more strongly destabilized relative to the atop site in going from bulk Pd to monolayer Pd. As a result, the atop site is the most stable adsorption site for CO on the supported Pd monolayer, while the three-hollow site is the most stable adsorption site for CO on bulk Pd. The presence of the NH_3 molecule, an electron donor, on the Pd_{1ML}/Mo(110) surface partially restores the adsorption behavior of bulk Pd with respect to CO. This again is due to electron donation from NH_3 to the surface and implies that the availability of electron density for back-donation in CO bonding to a transition-metal surface is the dominating factor in determining the adsorption site of CO.

Since both CO−CO and NH_3−NH_3 interactions are repulsive and the CO−NH_3 interaction is attractive, coadsorbed CO and NH_3 form mixed, rather than separate, domains. Even at the low coverage limit, a change in the bonding site of CO from atop to the 3-fold hollow, induced by coadsorbed NH_3 molecules, is consistent with the formation of a $(CO)^{8-}$−$(NH_3)^{8+}$ complex due to the attractive interaction between CO and NH_3.

5. Conclusion

Using NH_3 as a probe, the Pd monolayer has been shown to have a slightly reduced density of states near the Fermi level and thus is better able to accept electron density from NH_3 compared with the bulk-terminated Pd surface. These results together with previous results obtained for these systems show that monolayer Pd compared with bulk Pd has a more deficient density of state near the Fermi level. The results of NH_3 and CO coadsorption show an attractive interaction between these two molecules, a significantly modified characteristic vibrational mode, and a change in the CO adsorption site on the Pd_{1ML}/Mo(110) surface.

Acknowledgment. We acknowledge with pleasure the support of this work by the Department of Energy, Office of Basic Energy Sciences, Division of Chemical Sciences.

References and Notes

(1) Rodriguez, J. A. *Surf. Sci. Rep.* **1996,** *24*, 223.
(2) Bauer, E. *The Chemical Physics of Solid Surfaces and Heterogeneous Catalysis*; King, D. A., Woodruff, D. P., Eds.; Elsevier: Amsterdam, 1984.
(3) Campbell, C. T. *Annu. Rev. Phys. Chem.* **1990**, *41*, 775.
(4) Rodriguez, J. A.; Goodman, D. W. *Science* **1992**, *257*, 897.
(5) Rodriguez, J. A.; Campbell, R. A.; Goodman, D. W. *Surf. Sci.* **1994**, *377*, 307.
(6) Weng, S.-L.; El-Batanouny, M. *Phys Rev. Lett.* **1980**, *44*, 612.
(7) El-Batanouny, M.; Strongin, M.; Williams, G. P.; Colbert, J. *Phys. Rev. Lett.* **1981**, *46*, 269.
(8) Williams, G. P.; El-Batanouny, M.; Colbert, J.; Jensen, E.; Rhodin, T. N. *Phys. Rev.* **1982**, *B25*, 3658.
(9) Ruckman, M. W.; Johnson, P. D.; Strongin, M. *Phys. Rev.* **1985**, *B31*, 3405.
(10) Frick, B.; Jacobi, K. *Phys. Rev. B* **1988**, *37*, 4408.
(11) Koel, B. E.; Smith, R.; Berlowitz, P. J. *Surf. Sci.* **1990**, *231*, 325.
(12) Campbell, R.; Rodriguez, J.; Goodman, D. W. *Surf. Sci.* **1990**, *240*, 71.
(13) Heitzinger, J. M.; Gebhard, S. C.; Koel, B. E. *Surf. Sci.* **1992**, *275*, 209.
(14) Heitzinger, J. M.; Gebhard, S. C.; Koel, B. E. *Chem. Phys. Lett.* **1992**, *200*, 65.
(15) Sellidj, A.; Koel, B. E. *Surf. Sci.* **1993**, *281*, 223.
(16) Heitzinger, J. M.; Gebhard, S. C.; Koel, B. E. *J. Phys. Chem.* **1993**, *97*, 5327.
(17) Kuhn, W. K.; Szanyi, J.; Goodman, D. W. *Surf. Sci.* **1994**, *303*, 377.
(18) Xu, C.; Goodman, D. W. *Surf. Sci.* **1996**, *360*, 249.
(19) Rodriguez, J. A.; Kuhn, W. K.; Truong, C. M.; Goodman, D. W. *Surf. Sci.* **1992**, *271*, 333.
(20) Parmeter, J. E.; Wang, Y.; Mullins, C. B.; Weinberg, W. H. *J. Chem. Phys.* **1988**, *88*, 5225.
(21) Erley, W.; Ibach, H. *Surf. Sci.* **1982**, *119*, L357.
(22) Gland, G. L.; Kollin, E. B. *Surf. Sci.* **1981**, *104*, 478.
(23) Sexton, B. A.; Mitchell, G. E. *Surf. Sci.* **1980**, *99*, 523.
(24) Sexton, B. A.; Mitchell, G. E. *Surf. Sci.* **1980**, *99*, 539.
(25) Seabury, C. W.; Rhodin, T. N.; Purtell, R. J.; Merrill, R. P. *Surf. Sci.* **1980**, *93*, 117.
(26) Netzer, F. P.; Madey, T. E. *Phys. Rev. Lett.* **1981**, *47*, 928.
(27) Netzer, F. P.; Madey, T. E. *Surf. Sci.* **1982**, *119*, 422.
(28) Kang, W. M.; Li, C. H.; Tang, S. Y.; Seabury, C. W.; Jacobi, K.; Rhodin, T. N.; Purtell, R. J.; Merrill, R. P. *Phys. Rev. Lett.* **1981**, *47*, 931.
(29) Grunze, M.; Golze, M.; Driscoll, R. K.; Dowber, P. A. *J. Vac. Sci. Technol.* **1981**, *18*, 611.
(30) Jacobi, K.; Jensen, E. S.; Rhodin, T. N.; Merrill, R. P. *Surf. Sci.* **1981**, *108*, 397.
(31) Gland, J. L.; Sexton, B. A.; Mitchell, G. E. *Surf. Sci.* **1982**, *115*, 623.
(32) Ceyer, S. T.; Yates, J. T. *Surf. Sci.* **1985**, *155*, 584.
(33) Netzer F. P.; Madey, T. E. *Chem. Rev. Lett.* **1982**, *88*, 315.
(34) Wu, M. C.; Truong, C. M.; Goodman, D. W. *J. Phys. Chem.* **1993**, *97*, 4182.
(35) Tochihara, H.; Rocker, G.; Redding, J. D.; Yates, Jr., J. T.; Martin, R. M.; Metiu, H. *Surf. Sci.* **1986**, *176*, 1.
(36) Dresser, M. J.; Lanzillotto, A. M.; Alvey, M. D.; Yates, Jr., J. T. *Surf. Sci.* **1987**, *191*, 1.
(37) Lanzillotto, A. M.; Dresser, M. J.; Alvey, M. D.; Yates, Jr., J. T. *Surf. Sci.* **1987**, *191*, 15.
(38) Erley, W. *Surf. Sci.* **1990**, *240*, 1.
(39) Zhou, Y.; Akhter, S.; White, J. M. *Surf. Sci.* **1988**, *202*, 357.
(40) Sasaki, T.; Aruga, T.; Kuroda, H.; Iwasawa, Y. *Surf. Sci.* **1989**, *224*, L969.
(41) Rosenzweig, Z.; Asscher, M.; Wittenzellner, C. *Surf. Sci. Lett.* **1990**, *240*, 583.
(42) Lackey D.; King, D. A. *J. Chem. Soc., Faraday Trans.* **1987**, *83*, 2001.
(43) Mijoule, C.; Bouteiller, Y.; Salahub, D. R. *Surf. Sci.* **1991**, *253*, 375.
(44) Parmeter, J. E.; Jiang, X.; Goodman, D. W. *Surf. Sci.* **1990**, *240*, 85.
(45) Parker, Ch.; Bauer, E.; Poppa, H. *Surf. Sci.* **1985**, *154*, 371.
(46) Benndorf, C.; Madey, T. E. *Surf. Sci.* **1983**, *135*, 164.
(47) Hoffmann, F. M.; Lang, N. D.; Nørskov, J. K. *Surf. Sci. Lett.* **1990**, *226*, L48.
(48) Xu, Z.; Sherman, M. G.; Yates, Jr., J. T.; Antoniewicz, P. R. *Surf. Sci.* **1992**, *276*, 249.
(49) Zenobi, R.; Xu, J.; Yates, Jr., J. T. *Surf. Sci.* **1992**, *276*, 241.
(50) Xu, Z.; Surnev, L.; Uram, K. J.; Yates, Jr., J. T. *Surf. Sci.* **1993**, *292*, 235.